# Changes in DNA bending induced by restricting nucleotide ring pucker studied by weak alignment NMR spectroscopy

Zhengrong Wu[†‡], Melissa Maderia[§], Joseph J. Barchi, Jr.[§], Victor E. Marquez[§], and Ad Bax[†¶]

[†]Laboratory of Chemical Physics, National Institute of Diabetes and Digestive and Kidney Diseases, National Institutes of Health, Bethesda, MD 20892-0520; and [§]Laboratory of Medicinal Chemistry, Center for Cancer Research, National Cancer Institute, Frederick, MD 21702

Contributed by Ad Bax, November 18, 2004

**Changes in bending of the DNA helix axis caused by the introduction of conformationally locked nucleotide analogs into the center region of the palindromic Dickerson dodecamer, d(CGCGAATTCGCG)$_2$, have been studied by NMR measurement of residual one-bond $^{13}$C-$^1$H dipolar couplings. Thymidine analogs, in which the deoxyribose was substituted by bicyclo[3.1.0]hexane, were incorporated in the T7, T8, and T7T8 positions. These nucleotide analogs restrict the ring pucker to the C2′-exo or ''north'' conformation, instead of C2′-endo or ''south,'' which dominates in regular B-form DNA. For all three oligomers, bending toward the major groove is found relative to the native molecule. The effects are additive with bending of 5 ± 1° per locked nucleotide. Measurement of the change in bending is more accurate than measurement of the bending angle itself and requires far fewer experimental data.**

conformational change | liquid crystal | nucleic acid

There is much interest in the design of novel DNA oligomers that assume predefined structural features. A considerable variety of such synthetic oligodeoxynucleic acids, with chemical modifications in either the nucleobase or furanose portion of the nucleotide building blocks, have been studied through a wide range of biophysical techniques (1, 2). Because many of these analogues hybridize efficiently with RNA, they hold considerable therapeutic potential in antisense technologies, where regulation of specific gene translation may slow or halt the progression of disease. Preorganizing oligonucleotide structures to forms observed in complexes with, for example, transcription factors will also modulate the affinity of such complexes and thereby holds potential to regulate protein production at the level of transcription.

DNA's flexibility is generally believed to play a critical role in protein–DNA recognition and has been widely studied through both computational and experimental techniques (3–6). In protein–DNA complexes, any kink in the DNA axis frequently is accompanied by a change in deoxyribose ring pucker (7, 8) from its predominant C2′-endo (south, *S*) conformation to C3′-endo or C2′-exo (north, *N*). NMR has provided strong evidence that a dynamic *S*/*N* equilibrium preexists in standard B-form DNA but that it usually is strongly shifted toward *S* (9–11). The correlation between the presence of kinks and *N* conformations of deoxyribose implicates the dynamic switching in ring pucker as a factor contributing to DNA flexibility.

The inherent flexibility of DNA, and the fact that both *N* and *S* conformers are energetically accessible, makes the structure of *crystallized* oligomers particularly sensitive to a host of factors. These include intermolecular hydrogen bonding, cocrystallization agents, and the specific coordination of divalent cations that often have low occupancies under physiological solution conditions. Although x-ray diffraction studies of crystallized oligomers have provided pivotal insights into the factors governing local geometries in such molecules (12, 13), net bending of their helical axis is often dominated by conditions related to the crystalline form (14–16). The sequence dependence of DNA bending therefore has been studied primarily by indirect methods such as interpretation of anomalous gel shifting, or rates of cyclization. Conventional, nuclear Overhauser effect-based NMR spectroscopy can provide a precise view of local geometry in oligonucleotides (4, 5), but accumulation of small errors makes this approach ill suited for the study of more global properties such as DNA bending.

More recently, the introduction of dilute aqueous liquid crystalline media and anisotropically compressed polyacrylamide gels has made it possible to weakly align (on the order of $10^{-3}$) macromolecules such as DNA oligomers relative to an external magnetic field (17–20). Under conditions of weak alignment, residual dipolar couplings (RDCs) between proximate atomic nuclei can be measured by NMR spectroscopy (21, 22). They provide very precise information on the time-averaged orientation of the corresponding vectors relative to the magnetic field, and thereby on the bending of the helical axis. This technology has been applied to study a number of important structural nucleic acid problems, including bending associated with so-called A-tracts (23–25), the study of bends induced by bulges (26), measurement of the interhelix angles in a hammerhead ribozyme (27), and the assembly of large RNA oligomers from smaller substructures (28, 29).

The accuracy at which the average orientation of the helix axis of a short, double-stranded nucleic acid fragment can be determined relative to the magnetic field limits the precision at which helical bending can be derived from RDCs. In practice, determination of the average orientation of such a fragment often is limited by the accuracy of the coordinates of the local structure and not by the uncertainty in the measurement of the RDCs. The random, small errors in the vector orientations of chemical bonds in structures, derived by either x-ray crystallography or NMR spectroscopy, are commonly referred to as structural noise. Minimizing this structural noise by using the highest-quality reference structures increases the accuracy of the RDC-derived, time-averaged orientation of a local domain structure. Precise measurement of the absolute curvature of the helix axis then requires the precise measurement of as large as possible a set of RDCs, often relying on extensive isotopic enrichment procedures.

Although the absolute uncertainty in the NMR measurement of the relative orientation of two substructures or domains on the basis of RDCs is limited by structural noise (30), we here demonstrate that the effect of this noise largely cancels when measuring a change in relative domain orientation, caused by an outside factor such as a point mutation or a change in sample conditions. Therefore, *changes* in a global property such as DNA

Abbreviations: *N*, north; RDC, residual dipolar coupling; *S*, south; TROSY, transverse relaxation-optimized spectroscopy.

[‡]Present address: Department of Biochemistry, Ohio State University, Columbus, OH 43210.

[¶]To whom correspondence should be addressed. E-mail: bax@nih.gov.

 www.pnas.org/cgi/doi/10.1073/pnas.0408498102

bending, induced by a local structural perturbation, can be rapidly and accurately determined from a far more limited set of one-bond RDCs and are much less sensitive to structural noise than measurement of the helical axis bending itself. Acquiring the smaller subset of such RDCs is technically quite straightforward and may not even require the use of $^{13}C$ enrichment.

We demonstrate the approach for analogs of the palindromic *Eco*RI restriction site, d(CGCGAATTCGCG)$_2$, commonly known as the Dickerson dodecamer (31). For the center four base pairs, the structure of the natural dodecamer observed by x-ray diffraction is nearly identical to that obtained by liquid crystal NMR (11). Considerable differences in the flanking regions are attributed to the binding of divalent cations and to intermolecular hydrogen bonds in the crystalline state (32), and we therefore use the solution structure (11) as a reference. Measurement of changes in helix axis bending will be demonstrated for d(CGCGAATTCGCG)$_2$, "mutated" by substitution of its T nucleotides by thymidine analogs that contain a bicyclo[3.1.0]hexane instead of deoxyribose (33).

Measurement of small changes in long-range structure described herein is equally applicable to proteins, nucleic acids, and complex carbohydrates. A prerequisite for cancellation of the effect of structural noise is that the change in the time-averaged orientation of the domains relative to the magnetic field is much smaller than one radian, and that the local structure of the domains remains the same. This type of RDC analysis therefore provides a particularly accurate and convenient method to study changes in a quaternary structure induced by allosteric activation or binding of ligands in general.

## Materials and Methods

**Sample Preparation.** Dodecamers T7*, T8*, and T7*T8* were prepared as described in ref. 33, further purified by ethanol precipitation, resuspended in $H_2O$, adjusted to pH 7.0, and lyophilized. Samples for NMR analysis were then dissolved in $D_2O$ (10 mM phosphate buffer, pH 7.0), containing 2 mM EDTA, 50 mM KCl, and 0.04% $NaN_3$. Concentrations of the modified dodecamers were all ≈3 mM for the homodimer (determined by UV absorbance at 260 nm and fitting to Beer's Law, using $\varepsilon$ = 110,700 liters/mol·cm; see Biopolymer Calculator at http://paris.chem.yale.edu/extinct.html). All modified DNA samples contained 20 mg/ml Pf1 to induce alignment, using sample volumes of 0.230 $\mu$l in straight-walled Shigemi (Allison Park, PA) microcells for NMR analysis.

**NMR Data Collection.** NMR spectra were recorded at 800 MHz $^1H$ frequency (35°C), using a Bruker DRX800 NMR spectrometer. Two-dimensional transverse relaxation-optimized spectroscopy (TROSY) and anti-TROSY $^1H$-$^{13}C$ correlation spectra were acquired in an interleaved manner, using the pulse sequence of ref. 34. Spectra for the aromatic and sugar regions of the spectra were recorded separately, to accommodate the wide range in $^{13}C$ chemical shifts and $^1H$-$^{13}C$ scalar couplings. Each TROSY and anti-TROSY spectrum consisted of a 512* × 700* time domain matrix, with acquisition times of 63.8 ms ($t_2$) and 96 ms ($t_1$) (base, TROSY), 63.8 ms ($t_2$) and 48 ms ($t_1$) (base, anti-TROSY), and 63.8 ms ($t_2$) and 70.4 ms ($t_1$) (deoxyribose; both TROSY and anti-TROSY). Different $^{13}C$ spectral windows were used for the interleaved recording of the base TROSY and anti-TROSY correlations, to partially compensate for the fast decay of the anti-TROSY $^{13}C$ signal. NMR spectra were apodized by cosine-squared bell (F2) and 72°-shifted sine bell (F1) windows and zero filled to yield a digital resolution of 3.9 Hz ($^1H$) and 3.1 Hz ($^{13}C$, base TROSY), 6.1 Hz ($^{13}C$, base anti-TROSY), and 4.9 Hz ($^{13}C$, deoxyribose), before peak picking with NMRPIPE software (35).

## Results

The ring conformation of bicyclo[3.1.0]hexane nucleoside analogs corresponds to a furanose ring pucker that is tightly locked into the *N* region of conformational space (36). In this analog, one edge of the fused cyclopropane ring substitutes for the C4′–O4 bond (*Inset* in Fig. 1*B*). Here, we study three DNA oligomers, substituted in the T7, T8, and T7T8 positions by thymidine analogs containing this bicyclo[3.1.0]hexane. Below, these substituted double-stranded dodecamers are referred to as T7*, T8*, and T7*T8*. For T7*, $^1H$ and $^{13}C$ chemical shifts for base pairs C1:G24–G4:C21 (and thereby C9:G16–G12:C13) are nearly identical to those observed in the native dodecamer, indicating that the local structure of these flanking regions is not affected by the substitution. For the T8* and T7*T8* molecules, chemical shifts of base pairs C9:G16 (and G4:C21), which are adjacent to the modified base pairs, are affected, but those for the terminal three base pairs remain nearly unaltered. Considering that NMR chemical shifts are exquisitely sensitive to even minute changes in structure, we therefore may safely conclude that the structure of the terminal regions is essentially unaffected by modifications that are two or more base pairs removed. This observation also implies that corresponding isotropic one-bond $^{13}C$-$^1H$ splittings for the terminal base pairs are the same for all four oligonucleotides to within experimentally attainable precision, obviating the need to remeasure these isotropic $^1J_{CH}$ values for T7*, T8*, and T7*T8*. Then, fitting the measured RDCs to structures corresponding to the terminal regions of the native DNA yields direct information on their relative orientation, i.e., on bending imparted by the modifications.

$^{13}C$-$^1H$ RDCs are obtained from the difference in one-bond $^{13}C$-$^1H$ splitting observed in the absence and presence of Pf1 (19). As an example, Fig. 1 compares a small region of the 2D $^1H$-$^{13}C$ correlation spectrum of aligned T7* with the corresponding region of the native dodecamer under isotropic conditions. The change in the observed splittings yields the RDCs. Although the degree of spectral overlap in the four samples varies, primarily as a result of changes in resonance frequencies for the center four nucleotides, on average we measure about seven to eight RDCs per base pair, included as Table 3, which is published as supporting information on the PNAS web site.

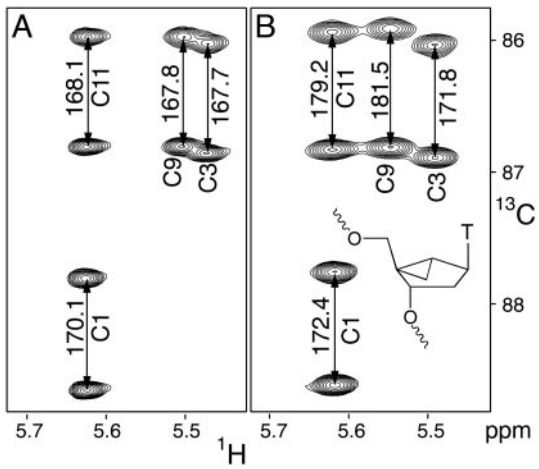


**Fig. 1.** Small sections of the overlayed 800-MHz TROSY and anti-TROSY 2D $^1H$-$^{13}C$ correlation spectra (42), recorded in interleaved mode at natural $^{13}C$ abundance for the native Dickerson dodecamer under isotropic conditions (*A*) and for T7* in the presence of 20 mg/ml Pf1 (*B*). Nucleotide assignments of the observed pairs of $C_{1'}$-$H_{1'}$ correlations and one-bond splittings (in Hz) are indicated. Methylene ($C_{2'}$; $C_{5'}$) signals are not observed in these TROSY spectra. The *Inset* in *B* depicts the bicyclo[3.1.0]hexane nucleoside analogue (T, thymine).

There are several ways to evaluate the changes in relative orientation of the two opposing ends of the oligomer from the experimental data. For small angle rotations, conceptually the easiest solution is to perform a 3D grid search, in which the top six base pairs of the original solution NMR structure (PDB entry 1NAJ) (11) are rotated about the principal $x$, $y$, and $z$ axes of the diagonalized alignment tensor by angles, $\alpha$, $\beta$, and $\gamma$, while keeping the bottom six base pairs fixed (Fig. 2). A singular value decomposition (SVD) fit of the dipolar couplings measured for the terminal three (or four for T7*) base pairs to each structure resulting from such rotations then provides a grid of SVD-goodness-of-fit results, where the minimum rms difference between measured and best-fitted couplings is obtained for $\alpha$, $\beta$, and $\gamma$ values that represent the bending about the $x$ and $y$ axes and the rotation about the $z$ axis, respectively, induced by the locked nucleotides.

Fig. 3 shows a contour diagram of a cross section through this ($\alpha$, $\beta$, $\gamma$) surface taken at $\gamma = 0°$. The contour diagram represents the rms difference between measured and best-fitted dipolar couplings. The lowest rms differences for the T7* and T8* molecules (2.0 and 2.1 Hz) are nearly the same as those for the native sequence, confirming that the structure of the terminal regions is unchanged. A small increase (to 2.9 Hz) for the T7*T8* molecule indicates that changes in the structure of its terminal 3-bp segments are just above the noise threshold, with corresponding very small chemical-shift changes ($\leq$0.07 ppm $^1$H) in base pairs C3:G22 and G10:C15.

The bend angle, $\alpha$, involves a rotation of the top part of the molecule about the $x$ axis of the molecular alignment tensor (Fig. 2) and therefore is tightly defined by the dipolar couplings.

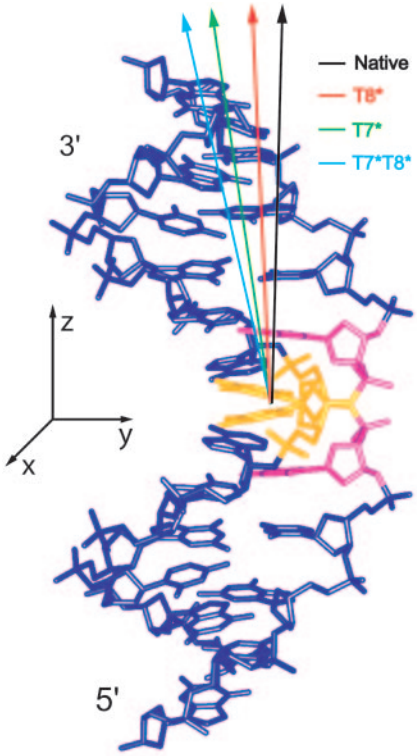


**Fig. 2.** Comparison of helical axis orientation for the top of the palindromic d(CGCGAATTCGCG)$_2$ sequence (black) with those in T7* (green), T8* (red), and T7*T8* (aqua), when keeping the bottom three (T8* and T7*T8*) or four (T7*) base pairs superimposed on the corresponding region in the native sequence. The $x$–$y$–$z$ frame corresponds to the principal axes of the d(CGCGAATTCGCG)$_2$ alignment tensor. T7 and T8 nucleotides of each strand are shown in orange and magenta, respectively.

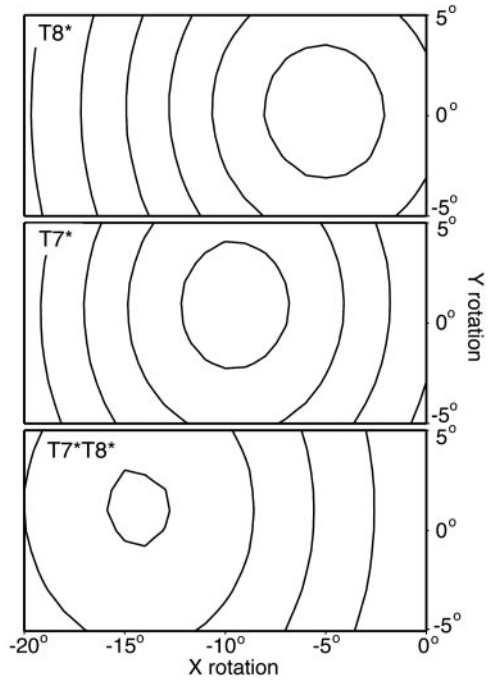


**Fig. 3.** Contour plot of the rms difference between dipolar couplings measured for the terminal three (T8*, T7*T8*) or four (T7*) base pairs, and those predicted by a SVD fit to a structure where the top half of the native Dickerson dodecamer structure (PDB entry 1NAJ) has been rotated relative to the bottom. Negative X rotations correspond to bending into the major groove (see Fig. 2). The lowest contour level corresponds to a rms difference of 2.2 Hz (T8*), 2.1 Hz (T7*), and 2.9 Hz (T7*T8*), with a factor 1.14 between successive contours.

Negative $\alpha$ values correspond to bending in the direction of the major groove. The angle $\beta$ refers to bending about the $y$ axis. However, this axis coincides with the $C_2$ symmetry axis of the palindromic molecules. Thus, the net bending about this axis would be zero if the structure were "noise free" or if $C_2$ symmetry had been imposed during calculation of the reference structure. Small deviations from the $\beta = 0°$ condition reflect the absence of perfect symmetry in the reference structure of the native dodecamer. Rotations of the top four base pairs about the $z$ axis ($\gamma$) result only in very small changes of predicted dipolar couplings because the alignment tensors are close to axially symmetric, and $\gamma$ is therefore poorly determined by the RDCs.

It is interesting to note that, within experimental error, the global bend angles found for T7*T8* correspond to the sum of the angles measured for T7* and T8* separately (Table 1). The results plotted in Fig. 3 show an increased bending of the oligonucleotide into the major groove when going from the native dodecamer to T8*, T7*, and T7*T8*. The modified

**Table 1. Bend angles of modified Dickerson dodecamers relative to the native sequence**

| DNA oligomer | $\alpha$, ° | $\beta$, ° | $\gamma$, ° |
|---|---|---|---|
| T7* | −9.8 ± 0.7[†] | 0.5 ± 1.0 | −6 ± 8 |
| T8* | −4.9 ± 0.8 | 0.0 ± 0.6 | −5 ± 6 |
| T7*T8* | −14.4 ± 0.8 | −1.0 ± 1.1 | −8 ± 6 |

[†]Reported uncertainties only take into account the effect of measurement error in the RDCs of the modified dodecamers, not the effect of structural noise. Angles reported correspond to Euler rotations of the 5′-terminal region relative to the 3′-terminal region of the native dodecamer, using the coordinate system of the diagonalized alignment tensor of the native dodecamer as the reference frame (Fig. 2).

nucleotide in T7* is present in adjacent base pairs T7:A18 and A6:T19. The long axes of these base pairs make angles of about ±18° with the $x$ axis of the alignment tensor, and bending effects of the T7 and T19 modifications therefore are nearly additive. In contrast, in the native Dickerson dodecamer, the A5:T20 and T8:A17 axes make angles of ± 54° with $x$, and the sum of the helix axis bending contributions around the $x$ axis scales with cos(54°) = 0.59. Therefore, the combined, net bending effect from modifications of the T8 and T20 nucleotides is expected to be scaled down by ≈40% compared with modifications in the T7 and T19 positions. This prediction is consistent with our experimental findings (Table 1).

In the native dodecamer, used as a reference in the present study, deoxyribose puckers are a dynamic average between *S* and *N*. For most purines, the equilibrium is shifted to nearly 100% *S*, but for pyrimidine nucleotides the percentage of *N* conformers is typically 15–20% (9, 37). The bend angles reported in Table 1 represent the difference between the dynamically averaged bend angle (80–85% *S*; 20–15% *N*) and the 100% *N* conformation, and therefore underestimate the net bending associated with a switch from *S* to *N* by ≈20%. The combined bending resulting from modifications in the T7 and T19 positions is 9.8°, or 5° per modified nucleotide. Accounting for the above-mentioned *S*/*N* equilibrium in the natural oligomer, this finding indicates that a switch in sugar from *S* to *N* is associated with a 6° bend into the major groove.

**Effect of Structural Noise and Internal Dynamics.** There are two, conceptually different methods for evaluating the uncertainty in the obtained $\alpha$, $\beta$, and $\gamma$ angles. Which method to use depends on which factor dominates the uncertainty of the resulting angles: errors in the measurement of the dipolar coupling or small random errors in the atomic coordinates of the reference structure. The error in the measured RDC value can be derived from reproducibility of multiple measurements or from analysis of the uncertainty in peak position based on the observed line width and signal-to-noise ratio (38). Mostly, these errors are smaller than ≈1 Hz (Table 3). Adding random, Gaussian-distributed noise to ideal RDCs, calculated for either the native or the bend structures while using experimentally observed alignment tensors, followed by refitting of these noise-contaminated data yields very small errors in the bend angles (Table 1).

As discussed previously, determination of the orientation of an alignment tensor for a molecule or molecular fragment is seldom dominated by the error in the RDC measurement itself but rather by the uncertainty in the atomic coordinates (30), often referred to as structural noise. The accuracy with which a given fragment can be oriented relative to the alignment tensor is then dominated by this structural noise. Below, we demonstrate that although the absolute value of the bend of the helix axis is dominated by this structural noise, the effect of structural noise largely cancels when measuring the differences in helical bending between similar structures, provided that the differences in bend angles are small (≤20°) and the orientation relative to the alignment tensor remains similar.

Considering that the NMR spectra of the terminal nucleotides of the native and modified oligomers are virtually indistinguishable, not only the local structure but also the dynamic properties of the terminal regions are very similar. The amplitudes of these local motions can be substantial, however. In the case of an overdetermined system, they decrease the attainable goodness-of-fit and cross-validation statistics (11), i.e., the accuracy at which the time-averaged coordinates of a structure can be determined. Cross-validation results previously obtained for the highest-resolution NMR structures indicate a considerable degree of structural noise resulting from internal dynamics for the native Dickerson dodecamer, on the order of 5–6° (11). We evaluate the effect of this structural uncertainty on the derived bend angles by adding Gaussian-distributed structural noise with a rms amplitude of 6° to the vector orientations in the reference structure (PDB entry 1NAJ). Twenty such models are generated, each with independent structural noise. In these models, bond vectors corresponding to measured couplings are redistributed randomly in cones around those of the reference structure, with a Gaussian probability function describing the angle between the original and noise-contaminated orientation (30).

Evaluation of the measured couplings for these noise-contaminated models, using only the small number of dipolar couplings measured in the terminal sections of the dodecamer, indicates a considerable spread in the bend angles. For the noise-contaminated reference structures, *averaged* over the 20 models, the helical axis bending relative to the original reference structures is close to zero, as expected. However, the rms variation in bending angles is ≈3° for $\alpha$ and 5° for $\beta$ (Table 2). Analogously, when using the same noise-contaminated structures to evaluate the bending angle for the three modified oligomers, relative large spreads are observed for both $\alpha$ (2–4°) and $\beta$ (≈4°) (Table 2). However, it is important to note that when for each noise-contaminated structure the difference in bending angle is calculated between the native and modified dodecamers, the rms spread in bending angle across the twenty structures is considerably lower (1.6° for $\alpha$; <3° $\beta$) (Table 2).

The partial cancellation of the effect of structural noise on bending angles, observed above, requires that the same set of RDCs is used for the two structures that are being compared. Because resonance overlap is different in the native and modified dodecamers, several RDCs could only be measured in one but not the other structure. To optimize cancellation of structural noise, these RDCs therefore were excluded from the analysis. It is also important to note that cancellation of the effect of structural noise is only effective when rearrangements relative to the alignment tensor frame are small. The twist about the $z$ axis of the alignment tensor is very sensitive to structural noise, resulting in $\gamma$ angle rms uncertainties in the reference structure as large as 24° and individual outliers as large as 80°. For such large values, the nonlinear dependence of dipolar couplings on orientation results in increasingly incomplete cancellation of the effect of structural noise. Even when considering the difference between the native and modified dodecamers, the rms uncertainty in the change in $\gamma$ therefore remains too large to allow any

**Table 2. Effect of structural noise on relative orientations and changes therein of the terminal regions of native and modified Dickerson dodecamers**

| DNA oligomer | $\alpha$, ° | $\beta$, ° | $\gamma$, ° |
|---|---|---|---|
| Native† | 1.3 ± 3.2 | 1.0 ± 5.0 | −1 ± 14 |
| T8* | −2.4 ± 3.9 | 0.6 ± 3.8 | 10 ± 10 |
| T8*-native† | −3.7 ± 1.6 | −0.5 ± 2.9 | 11 ± 15 |
| Native† | 0.6 ± 3.0 | 1.3 ± 5.3 | 11 ± 22 |
| T7* | −8.6 ± 1.9 | 1.8 ± 3.8 | 2 ± 13 |
| T7*-native‡ | −9.3 ± 1.7 | 0.5 ± 2.7 | −9 ± 12 |
| Native† | 1.6 ± 3.2 | 1.6 ± 4.7 | 3 ± 24 |
| T7*T8* | −12.7 ± 3.5 | 0.9 ± 3.8 | 17 ± 9 |
| T7*T8*-native‡ | −14.2 ± 1.6 | −0.7 ± 3.0 | 14 ± 22 |

†Average and standard deviation of RDC-derived rotation angles between the terminal domains of the structure of the native dodecamer (PDB entry 1NAJ) and a set of 20 noise-contaminated reference structures. Only RDCs in the terminal three base pairs (terminal four base pairs for T7*) that were measured in both the native and modified oligomer are used to define the rotation angles.

‡Average and standard deviation of pairwise difference in rotation angles obtained from data measured for modified and native dodecamers, for a set of 20 noise-contaminated reference structures.

definitive conclusions on the effect of the mutations on the change in helical twist (Table 2).

## Discussion

The observed degree of alignment, after correction for minor differences in applicable Pf1 concentration, is indistinguishable for the native and modified dodecamers. Moreover, the melting temperatures of the native dodecamer and its three analogs differ by <3°C, and there are no indications of structural abnormalities (e.g., bulges) in the modified helices. These observations rule out any significant change in large-scale dynamic properties between the native and modified dodecamer.

The amplitude of fluctuations in the helical bending parameters of B form DNA can be estimated from the dynamic persistence length of double-stranded DNA, estimated to be ≈800 Å (39) or 240 bp, which is considerably longer than the commonly used apparent persistence length of ≈500 Å (40). A dynamic persistence length of 240 bp corresponds to a random bending contribution of ≈4° per base pair, nearly double that estimated for the effect from sugar switching alone (when taking into account the skewed $S/N$ equilibrium). Dependent on ionic strength and the presence of $Mg^{2+}$, the dynamic persistence length of RNA is considerably longer than for DNA (41). Ribose sugars in double-stranded A-form RNA are not subject to the dynamic ring pucker switching observed in DNA and are normally tightly locked into the $N$ conformation. The longer RNA dynamic persistence length is therefore consistent with our finding that assigns the dynamic switching in deoxyribose ring pucker as a significant factor underlying DNA flexibility.

Although precise determination of the relative orientation of two domains, such as the terminal regions of the dodecamer considered in the present study, requires a very extensive set of dipolar-coupling measurements, small differences between closely related systems can be obtained accurately from far fewer data, provided that reasonable quality domain structures are available. For the Dickerson dodecamer, the solution structure of the terminal regions is known in detail from previous extensive liquid crystal NMR studies (11, 32). This system is therefore ideally suited to study the effect on helical bending of any nucleic acid sequence intervening between these two terminal regions. For longer intervening sequences, it will be helpful to use selective isotopic $^{13}C$ enrichment of the terminal domains only, whereas natural abundance measurements suffice for smaller systems such as those studied here.

Partial cancellation of the effect of structural noise when studying differences in domain orientations by liquid crystal NMR applies to all systems where the changes are modest. This approach therefore provides an exquisitely sensitive method to study small changes in quaternary structure induced by a wide range of factors, including allosteric activation of proteins, point mutations in hinge regions, and ligand binding.

We thank Frank Delaglio, Dennis A. Torchia, and Victor Zhurkin for useful discussions and Markus Zweckstetter for assistance in using the program PALES for adding Gaussian structural noise to the reference structure.

1. Kool, E. T. (2002) *Acc. Chem. Res.* **35,** 936–943.
2. Herdewijn, P. (1999) *Biochim. Biophys. Acta* **1489,** 167–179.
3. Young, M. A. & Beveridge, D. L. (1998) *J. Mol. Biol.* **281,** 675–687.
4. Metzler, W., Wang, C., Kitchen, D., Levy, R. & Pardi, A. (1990) *J. Mol. Biol.* **214,** 711–736.
5. Ulyanov, N. B., Gorin, A. A., Zhurkin, V. B., Chen, B. C., Sarma, M. H. & Sarma, R. H. (1992) *Biochemistry* **31,** 3918–3930.
6. Crothers, D. M. (1998) *Proc. Natl. Acad. Sci. USA* **95,** 15163–15165.
7. Rice, P. A., Yang, S. W., Mizuuchi, K. & Nash, H. A. (1996) *Cell* **87,** 1295–1306.
8. Tolstorukov, M. Y., Jernigan, R. L. & Zhurkin, V. B. (2004) *J. Mol. Biol.* **337,** 65–76.
9. van Wijk, J., Huckriede, B. D., Ippel, J. H. & Altona, C. (1992) *Method Enzymol.* **211,** 286–307.
10. Tonelli, M. & James, T. L. (1998) *Biochemistry* **37,** 11478–11487.
11. Wu, Z., Delaglio, F., Tjandra, N., Zhurkin, V. B. & Bax, A. (2003) *J. Biomol. NMR* **26,** 297–315.
12. Dickerson, R. E. (1983) *J. Mol. Biol.* **166,** 419–441.
13. Shui, X. Q., Sines, C. C., McFail-Isom, L., VanDerveer, D. & Williams, L. D. (1998) *Biochemistry* **37,** 16877–16887.
14. Dickerson, R. E., Goodsell, D. S., Kopka, M. L. & Pjura, P. E. (1987) *J. Biomol. Struct. Dyn.* **5,** 557–579.
15. DiGabriele, A. D., Sanderson, M. R. & Steitz, T. A. (1989) *Proc. Natl. Acad. Sci. USA* **86,** 1816–1820.
16. Dickerson, R. E., Goodsell, D. S. & Neidle, S. (1994) *Proc. Natl. Acad. Sci. USA* **91,** 3579–3583.
17. Tjandra, N. & Bax, A. (1997) *Science* **278,** 1111–1114.
18. Clore, G. M., Starich, M. R. & Gronenborn, A. M. (1998) *J. Am. Chem. Soc.* **120,** 10571–10572.
19. Hansen, M. R., Mueller, L. & Pardi, A. (1998) *Nat. Struct. Biol.* **5,** 1065–1074.
20. Tycko, R., Blanco, F. J. & Ishii, Y. (2000) *J. Am. Chem. Soc.* **122,** 9340–9341.
21. Bax, A. (2003) *Protein Sci.* **12,** 1–16.
22. Prestegard, J. H., Bougault, C. M. & Kishore, A. I. (2004) *Chem. Rev.* **104,** 3519–3540.
23. MacDonald, D., Herbert, K., Zhang, X. L., Polgruto, T. & Lu, P. (2001) *J. Mol. Biol.* **306,** 1081–1098.
24. Barbic, A., Zimmer, D. P. & Crothers, D. M. (2003) *Proc. Natl. Acad. Sci. USA* **100,** 2369–2373.
25. Stefl, R., Wu, H. H., Ravindranathan, S., Sklenar, V. & Feigon, J. (2004) *Proc. Natl. Acad. Sci. USA* **101,** 1177–1182.
26. Al-Hashimi, H. M., Gosser, Y., Gorin, A., Hu, W. D., Majumdar, A. & Patel, D. J. (2002) *J. Mol. Biol.* **315,** 95–102.
27. Bondensgaard, K., Mollova, E. T. & Pardi, A. (2002) *Biochemistry* **41,** 11532–11542.
28. Lukavsky, P. J., Kim, I., Otto, G. A. & Puglisi, J. D. (2003) *Nat. Struct. Biol.* **10,** 1033–1038.
29. D'Souza, V., Dey, A., Habib, D. & Summers, M. F. (2004) *J. Mol. Biol.* **337,** 427–442.
30. Zweckstetter, M. & Bax, A. (2002) *J. Biomol. NMR* **23,** 127–137.
31. Dickerson, R. E. & Drew, H. R. (1981) *J. Mol. Biol.* **149,** 761–786.
32. Tjandra, N., Tate, S., Ono, A., Kainosho, M. & Bax, A. (2000) *J. Am. Chem. Soc.* **122,** 6190–6200.
33. Maier, M. A., Choi, Y., Gaus, H., Barchi, J. J., Marquez, V. E. & Manoharan, M. (2004) *Nucleic Acids Res.* **32,** 3642–3650.
34. Weigelt, J. (1998) *J. Am. Chem. Soc.* **120,** 10778–10779.
35. Delaglio, F., Grzesiek, S., Vuister, G. W., Zhu, G., Pfeifer, J. & Bax, A. (1995) *J. Biomol. NMR* **6,** 277–293.
36. Marquez, V. E., Ezzitouni, A., Russ, P., Siddiqui, M. A., Ford, H., Feldman, R. J., Mitsuya, H., George, C. & Barchi, J. J. (1998) *J. Am. Chem. Soc.* **120,** 2780–2789.
37. Bax, A. & Lerner, L. (1988) *J. Magn. Reson.* **79,** 429–438.
38. Kontaxis, G., Clore, G. M. & Bax, A. (2000) *J. Magn. Reson.* **143,** 184–196.
39. Bednar, J., Furrer, P., Katritch, V., Stasiak, A. Z., Dubochet, J. & Stasiak, A. (1995) *J. Mol. Biol.* **254,** 579–591.
40. Hagerman, P. J. (1988) *Annu. Rev. Biophys. Biophys. Chem.* **17,** 265–286.
41. Hagerman, P. J. (1997) *Annu. Rev. Biophys. Biomol. Struct.* **26,** 139–156.
42. Pervushin, K., Riek, R., Wider, G. & Wuthrich, K. (1998) *J. Am. Chem. Soc.* **120,** 6394–6400.